

Reconstruction of Crack Shapes From the MFLT Signals by Using a Rapid Forward Solver and an Optimization Approach

Zhenmao Chen, Gabriel Preda, Ovidiu Mihalache, and Kenzo Miya

Abstract—In this paper, the reconstruction of crack shapes from the magnetic flux leakage testing (MFLT) signals is realized by introducing a rapid forward simulator and applying a deterministic optimization approach. The MFLT signals due to cracks of different shape are calculated with an FEM-BEM code employing A method and polarization algorithm, which is accelerated by the new rapid forward scheme. For reconstructing the crack shape, the conjugate gradient method is applied with the gradients predicted by using the difference technique. Both inner and outer crack are successfully reconstructed from simulated MFLT signals that verified both the efficiency of the fast-forward scheme and the feasibility of the deterministic inverse approach.

Index Terms—Deterministic methods, fast-forward scheme, inverse problems, nondestructive testing.

I. INTRODUCTION

SHAPE reconstruction of cracks in a structural component of magnetic material from the magnetic flux leakage testing (MFLT) signals is still a challenging subject because of the difficulties on the simulation of the nonlinear magnetic problem. Based on an assumption that the magnetization in the material has a uniform distribution, the authors of [1] have established an inverse scheme based on a magnetic dipole model. Unfortunately, this theory is not valid for MFLT with a small magnetizer. For treating the case with a distributed magnetization, a neural network approach has been applied to the shape reconstruction of cracks in [2], where measured data were used in the training of neural networks. In [3], the gradient-descent procedure has been employed in the inversion of the crack shape while the forward analysis is performed with the neural network approach for tackling the computational burden problem of a normal FEM code. Recently, a numerical code has been developed by the authors for simulating the static MFLT signals based on the FEM-BEM hybrid method [4] and the polarization approach [5]. However, this code is also difficult to be applied to MFLT inversion because of the computational burden issue. To overcome this difficulty, a scheme capable to reduce the numerical analysis region is proposed in this paper. Based on this scheme, one can significantly reduce the CPU time necessary in the crack signal simulation, and further, apply it to the crack

reconstruction. In the inverse procedure, the conjugate gradient (CG) method [6] of deterministic strategy is applied with the gradients calculated with the difference procedure. Numerical results show that the CG method can give a good prediction of the true crack shape in a few iteration steps. Even in addition with the computational time required for the gradient calculation, the inversion can be carried out in an acceptable CPU time.

II. SCHEME OF THE FAST MFLT SIGNAL SIMULATOR

A. Introduction of the FEM–BEM Polarization Method

For a static nonlinear electromagnetic problem, the governing equations can be written as follows by transforming the Maxwell equations with use of the magnetic vector potential and separating out the nonlinear part (magnetization \mathbf{M}) from the magnetic flux density [4]

$$\frac{1}{\mu_0} \nabla^2 \mathbf{A} = \nabla \times \mathbf{M}, \quad (\text{in material}) \quad (1)$$

$$\frac{1}{\mu_0} \nabla^2 \mathbf{A} = -\mathbf{J}_0, \quad (\text{in air}) \quad (2)$$

where \mathbf{A} is the magnetic vector potential defined by $\mathbf{B} = \nabla \times \mathbf{A}$. The constitutive relation between the magnetization vector \mathbf{M} and the magnetic flux density vector \mathbf{B} is as follows:

$$\mathbf{M} = \frac{1}{\mu_0} \mathbf{B} - \mathbf{F}(\mathbf{B}) \quad (3)$$

with function $\mathbf{F}(\mathbf{B})$ representing the nonlinear property of the ferromagnetic material.

Equations (1)–(3) can be solved by using the FEM-BEM discretization and the polarization method [5], [7]. The basic idea of the FEM–BEM hybrid method is to discretize the governing equation in material with FEM, the equation in air with the BEM and to couple the system equations with use of the following boundary equations:

$$\mathbf{A}|_{\text{fem}} = \mathbf{A}|_{\text{bem}} \quad (4)$$

$$\frac{1}{\mu_0} \frac{\partial \mathbf{A}}{\partial \mathbf{n}} - \mathbf{M} \times \mathbf{n} \Big|_{\text{fem}} = \frac{1}{\mu_0} \frac{\partial \mathbf{A}}{\partial \mathbf{n}} \Big|_{\text{bem}} \quad (5)$$

After discretization, one can obtain the system equations as

$$[K]\{A\} = [S]\{M\} + \{F\} \quad (6)$$

with $[K]$, $[S]$ being the coefficient matrices and $\{F\}$ the vector corresponding to the exciting current.

Equation (6) needs to be solved together with the nonlinear constitute relation (3). This typical nonlinear problem can be solved by using the polarization method that treats the magne-

Manuscript received July 1, 2001; revised October 25, 2001.

Z. Chen, G. Preda, and K. Miya are with the International Institute of Universality, Tokyo, 113-0031, Japan (e-mail: chen@jsaem.gr.jp).

O. Mihalache was with the Nuclear Engineering Research Laboratory, the University of Tokyo, Tokyo, Japan. He is now with the Plant Technology Development Group, International Cooperation and Technology Development Center, Inc., Fukui 919-1279, Japan.

Publisher Item Identifier S 0018-9464(02)02781-4.

tization term $[S]\{M\}$ as an external source, and solving it with a fixed-point procedure [5].

B. Fast Scheme for Predicting MFLT Signal

For an inspection object with a crack, the MFLT signal perturbation due to the crack can be calculated with the formula described above by solving the flawed and unflawed fields separately. To apply this strategy to the inverse analysis, however, a heavy computer burden is required, as a large number of forward analyses must be solved during the inversion. In this part, a fast-forward strategy is introduced for predicting the perturbation of MFLT signals which enables a great reduction of CPU time without losing numerical accuracy [8].

Referring to (1) and (2), the governing equations for an unflawed inspection object can be written as follows by denoting $\mathbf{A}^u, \mathbf{M}^u$ as the magnetic vector's potential and magnetization vector of the unflawed material

$$\frac{1}{\mu_0} \nabla^2 \mathbf{A}^u = \nabla \times \mathbf{M}^u, \quad (\text{in material}) \quad (7)$$

$$\frac{1}{\mu_0} \nabla^2 \mathbf{A}^u = -\mathbf{J}_0, \quad (\text{in air}). \quad (8)$$

In this case, constitute relation (3) also needs to be fulfilled.

Subtracting (7) and (8) from (1) and (2), one can obtain

$$\frac{1}{\mu_0} \nabla^2 \mathbf{A}^f = \nabla \times \mathbf{M}^f, \quad (\text{in material}) \quad (9)$$

$$\frac{1}{\mu_0} \nabla^2 \mathbf{A}^f = 0, \quad (\text{in air}) \quad (10)$$

where $\mathbf{A}^f = \mathbf{A} - \mathbf{A}^u$ is the difference of the vector potential and $\mathbf{M}^f = \mathbf{M} - \mathbf{M}^u$ is the difference of the magnetization vectors for cases with and without a crack.

Discretizing (9) with FEM, (10) with BEM, and coupling the discretized equations with the boundary conditions (4) and (5), one can obtain the discretized system equations as

$$[K]\{A^f\} = [S]\{M^f\} \quad (11)$$

where $[K]$ and $[S]$ are the coefficient matrices again. It is easy to find that the coefficient matrices $[K], [S]$ of the system (11) are the same as those appeared in (6) if the geometry and the material property of the inspection system are the same.

Usually, as the perturbation of the magnetic field due to a crack is significant only at the vicinity of the crack, one does not need to solve (9) and (10) at the whole analysis region for (1) and (2). This characteristic gives us the possibility of greatly reducing the computational time by choosing a smaller analysis region. However, as $\mathbf{B}^u, \mathbf{M}^u$ are necessary in (3), the magnetization distribution in the unflawed material is indispensable for solving (11), i.e., a calculation to obtain the unflawed field data has to be done in advance in order to take the reduced analysis region. Fortunately, for calculating the signal perturbation due to cracks of different shape, the unflawed magnetic field only need to be calculated one time as it is unrelated with the crack shapes. This feature is a key factor enabling the present strategy to be applied to the MFLT signal calculation for cracks in updating which is indispensable in the inverse analysis of both the deterministic and the AI approaches.

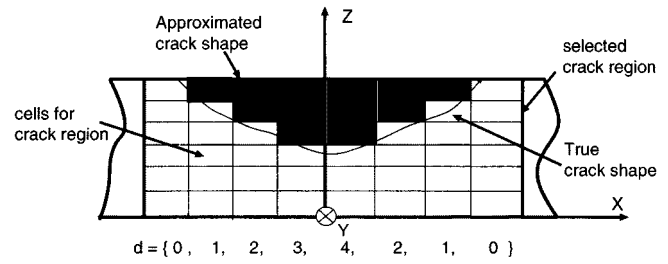


Fig. 1. Parameterization of the crack shape.

C. Numerical Implementation

In practice, a MFLT signal can be rapidly calculated with the following procedure.

- Step 1) Calculate the unflawed magnetic potential \mathbf{A}^u , magnetization \mathbf{M}^u , and the magnetic field \mathbf{B}^u with a conventional nonlinear analysis code, and storing them into a database.
- Step 2) Choose a smaller analysis region in the vicinity of the crack and discretizing it with the FEM-BEM strategy. In addition, inputting the database constructed in Step 1 and calculating $\mathbf{M}^u, \mathbf{B}^u$ at each node through interpolation.
- Step 3) Set the initial magnetization \mathbf{M}^f as $-\mathbf{M}^u$ for the node belonging to the crack elements and "0.0" for the other nodes.
- Step 4) Solve \mathbf{A}^f with (11), and calculate \mathbf{B} from the obtained \mathbf{A}^f through $\mathbf{B} = \mathbf{B}^f + \mathbf{B}^u$.
- Step 5) Calculate the magnetization \mathbf{M}^f from the magnetic field \mathbf{B} with use of the $B - H$ relation and $\mathbf{M}^f = \mathbf{M} - \mathbf{M}^u$. For a crack element, however, setting the magnetization as $\mathbf{M}^f = -\mathbf{M}^u$ again.
- Step 6) Calculate residual $E = |\mathbf{M}^n - \mathbf{M}^{n-1}|$.
- Step 7) If E is less than the selected threshold error, go to step 8. If not, jump back step 4.
- Step 8) Calculate the perturbation of the magnetic flux leakage from the perturbation of magnetization \mathbf{M}^f through $\mathbf{B}^f = \mu_0/4\pi \int_{\Omega} \nabla \times \mathbf{M}^f \times \nabla(1/R)dv + \mu_0/4\pi \int_{\Sigma} \mathbf{M}^f \times \mathbf{n} \times \nabla(1/R)ds$.

III. SCHEME OF INVERSE ANALYSIS

A. Parameterization of the Crack Shape

A crack [e.g., a stress corrosion crack (SCC)] in a structural component usually has a very complicated geometry. However, most of the cracks are in either the axial or the circumferential direction, and also nearly in a planar shape for a crack with a relative large size. As the first step to reconstruct natural crack with MFLT signal, we take an axial artificial (EDM) crack of planar shape with known crack opening and out-plane location as the target of this paper. As the input signal of the inversion, the MFLT signal ($b_i, i = 1, 2, \dots, m$) scanned along the crack line with a liftoff of 0.5 mm will be considered.

To solve this inverse problem, we suppose that we know the area where the crack possibly exists. Fig. 1 shows a selected region of crack plane that was subdivided into n subregions along the crack line. The depths of the crack in each subregion

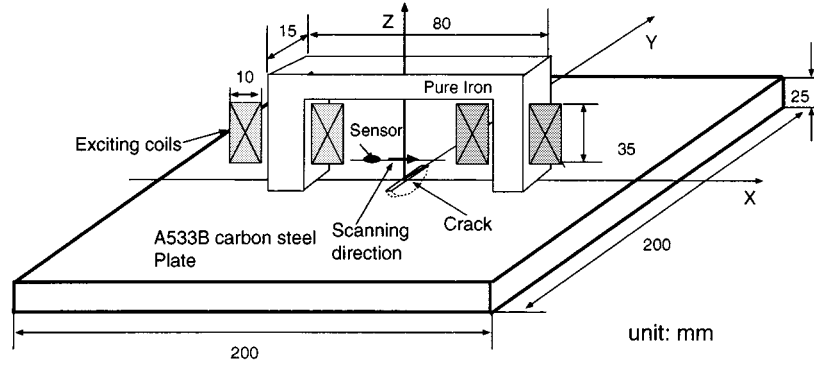


Fig. 2. Analysis model of the MFLT system.

$(d_j, j = 1, 2, \dots, n)$ will be taken as the crack parameters to be reconstructed.

B. Algorithm for Crack Shape Reconstruction

The crack parameters vector \mathbf{d} are reconstructed from the measured MFLT signals \mathbf{b}^{obs} by minimizing the objective function ε with use of a deterministic optimization approach, e.g., the CG method. In this work, the objective function is defined as,

$$\varepsilon = \sum_i (b_i(\mathbf{d}) - b_i^{\text{obs}})^2, \quad (12)$$

where, $b_i(\mathbf{d})$ is the simulated MFLT signal with the forward solver for a crack with a shape defined by parameter \mathbf{d} .

Following the procedure of CG method, the crack parameter vector can be solved with the following iteration algorithm:

$$\{d^n\} = \{d^{n-1}\} + a\{\partial\varepsilon/\partial d\} \quad (13)$$

where

$$\partial\varepsilon/\partial d_j = \sum_i 2(b_i(\mathbf{d}) - b_i^{\text{obs}}) \partial b_i / \partial d_j \quad (14)$$

is a component of the gradient of the objective function, and a is the step length parameter which can be obtained with the following formula:

$$a = - \sum_i^n \left[(b_i(\mathbf{d}) - b_i^{\text{obs}}) \frac{\partial b_i}{\partial a} \right] / \sum_i^n \left\{ \frac{\partial b_i}{\partial a} \right\}^2 \quad (15)$$

with

$$\partial b_i / \partial a = \sum_j^n \partial b_i / \partial d_j \cdot \partial\varepsilon / \partial d_j. \quad (16)$$

The derivatives $\partial b_i / \partial d_j$ are calculated with the difference method as

$$\partial b_i / \partial d_j = [b_i(\mathbf{d}) - b_i(\mathbf{d} + \delta d_j \mathbf{n}_j)] / \delta d_j \quad (17)$$

where $b_i(\mathbf{d})$ and $b_i(\mathbf{d} + \delta d_j \mathbf{n}_j)$ are calculated separately with the forward solver. \mathbf{n}_j is the unit vector along d_j direction. Usually, δd_j is chosen as the thickness of the layers subdividing the inspected plate.

C. Some Other Speed Up Techniques

From the previous section, it is easy to see that the coefficient matrix $[K]$ in (11) does not change during the nonlinear iteration as the magnetization term is in the right hand of the equation. This allows us to invert the matrix $[K]$ and store it at the first iteration. This inversion of the matrix can be applied directly in the later iterations.

On the other hand, as the crack parameter does not change significantly in case of the gradient calculation, the distribution of the magnetization of the unperturbed case can be used as the initial values of the perturbed problem. This treatment can reduce the number of iteration significantly for a given accuracy level.

IV. NUMERICAL RESULTS

A. Numerical Results of the Fast-Forward Solver

The problem shown in Fig. 2 is taken as an example to validate the proposed schemes. Two coils (1000 AT in each) are set to the yoke legs to produce a large external magnetic field. The flux leakage signals between the yoke poles are calculated (-10 to 10 mm). The sizes of the yoke, plate, and the coil are given in Fig. 2.

For calculating the database of unflawed field, the plate and the yoke are subdivided into a mesh of $29 \times 34 \times 8$ elements and $4 \times 4 \times 21$ elements respectively. The total number of the nodes is 10,000. Around 3 h of CPU time and 1.9 G of memory are required to get one solution (VT-alpha6). A crack of OD50% depth, 8-mm length, and a 0.5-mm opening is taken as the crack to be detected. Three cubic regions with different size are considered as the reduced analysis areas. The size and the mesh division are separately: Case 1: 12 mm \times 20 mm \times 25 mm, 11 \times 20 \times 8 (1760) elements; Case 2: 16 mm \times 24 mm \times 25 mm, 13 \times 22 \times 8 (2288) elements; and Case 3: 20 mm \times 28 mm \times 25 mm, 15 \times 24 \times 8 (2880) elements. For the reduced system, the yoke and the coil are not necessary to be considered. In Fig. 3, results of the full system and the normal FEM-BEM code are compared with those using the rapid forward scheme. The CPU times are, respectively, 3 min, 5 min, and around 8 min for the three reduced systems. From Fig. 3, one can find that the results of the fast-forward solver approach those of the full system when the reduced analysis region gets larger. However, even for the

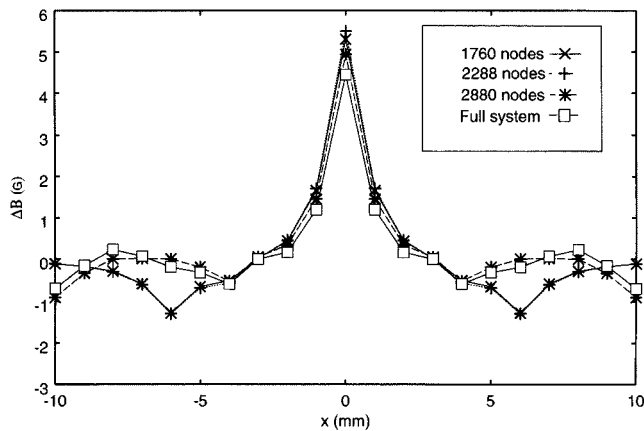


Fig. 3. Comparison of crack signals (B_x) along line $y = 0, z = 0.5$ calculated with the full system and the reduced regions.

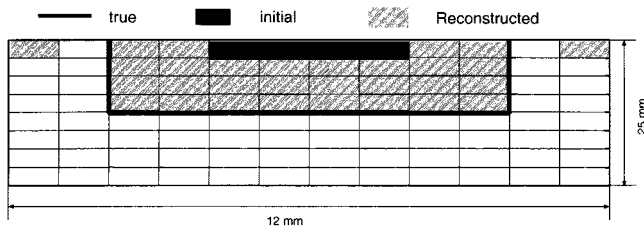


Fig. 4. Comparison of reconstructed and true crack shapes.

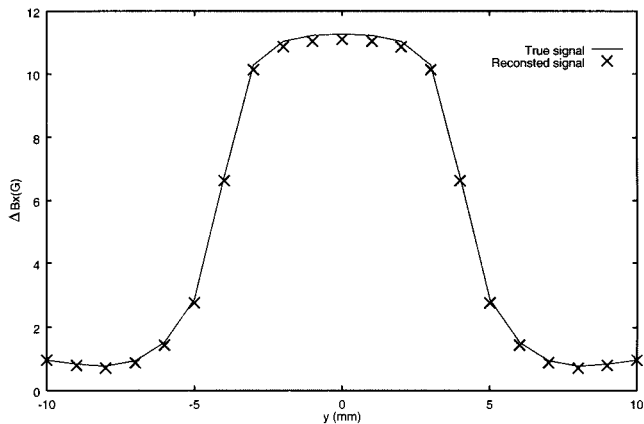


Fig. 5. Comparison of true MFL signal and those due to the crack of reconstructed shape.

smallest block region in the three cases, the maximum error is about 10%. These results proved that the proposed fast scheme is acceptable from the point of views of both the calculation speed and the analysis accuracy.

B. Numerical Results of Inverse Analysis

Fig. 4 shows an example of reconstruction results obtained by using the inversion scheme described in Section III. The true crack is an ID50% crack with a 0.5-mm opening and 8 mm in length. After about ten iterations, an acceptable reconstruction result was obtained. Fig. 5 gives a comparison of the true MFLT signals and those calculated with use of the crack in re-

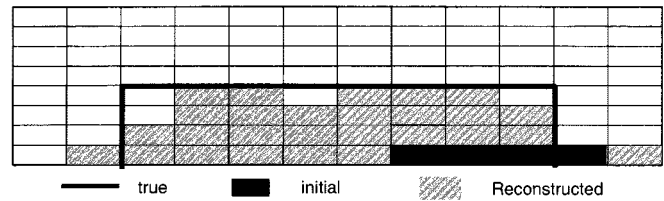


Fig. 6. Comparison of the true and the reconstructed crack shape for an OD crack.

constructed shape. Good agreement is also obtained. The total CPU time for obtaining the results shown in Fig. 4 is about 30 min. Fig. 6 gives a comparison of the reconstruction results for an OD crack. In this case, the input signal was used as the simulated MFLT signal of an OD 50% crack but with 10% white noise. The opening and the length of the crack were used as 0.5 and 8 mm again. From this result, one can see that a good reconstruction result can be obtained, even for a noise-polluted signal and an OD crack.

V. CONCLUSION

In this paper, a scheme for fast-forward simulation of the MFLT signals is proposed and was applied to the reconstruction of the crack shape with use of a deterministic optimization approach. The numerical results show that the fast-forward solver has both high accuracy and high simulation speed. It is also found that the inversion of the noise-polluted simulation signals can be performed by the deterministic approach in an acceptable computational time, which proved the validity and the efficiency of the inverse scheme using the fast-forward solver. As a next work, the validation of the proposed method in the analysis of the experimental data will be performed in the near future.

REFERENCES

- [1] D. Minkov and T. Shoji, "Sizing of 3-D surface cracks by using Hall element probe," in *Electromagnetic Nondestructive Evaluation*, D. Les-selier and A. Razek, Eds., 1998, pp. 283–291.
- [2] F. Katragadda, J. T. Si, E. Load, Y. S. Sun, S. Udpa, and L. Udpa, "Alternative magnetic flux leakage modalities for pipe line inspection," in *Proc. QNDE*, vol. 15, 1996, p. 561.
- [3] P. Ramuhalli, L. Udpa, and S. Udpa, "Neural network algorithm for electromagnetic NDE signal inversion," in *Electromagnetic Nondestructive Evaluation (V)*, J. Pavo, G. Vertesy, T. Takagi, and S. S. Udpa, Eds. Amsterdam, The Netherlands: IOS Press, 2000, pp. 121–128.
- [4] O. Mihalache *et al.*, "Crack reconstruction in ferromagnetic materials using nonlinear FEM-BEM scheme and neural networks," in *Electromagnetic Nondestructive Evaluation (V)*, J. Pavo, G. Vertesy, T. Takagi, and S. S. Udpa, Eds. Amsterdam, The Netherlands: IOS Press, 2000, pp. 67–74.
- [5] F. I. Hantila, G. Preda, and M. Vasiliu, "Polarization method for static fields," *IEEE Trans. Magn.*, vol. 36, pp. 672–675, May 2000.
- [6] Z. Chen and K. Miya, "ECT inversion using a knowledge based forward solver," *J. Nondestr. Eval.*, vol. 17, no. 3, pp. 157–165, 1998.
- [7] J. Fetzer, S. Kurtz, and G. Lehner, "Comparison of analytical and numerical integration techniques for the boundary integrals in the BEM-FEM coupling considering TEAM workshop problem no. 13," *IEEE Trans. Magn.*, vol. 33, pp. 1227–1230, Mar. 1996.
- [8] Z. Badics *et al.*, "Accurate probe response calculation in eddy current NDE by finite element method," *J. Nondestr. Eval.*, vol. 14, no. 3, 1995.